Optimizing Displacement-Based Seismic Design of Mass Timber Rocking Walls using Genetic Algorithm

Da Huang*, Shiling Pei, Aleesha Busch

Department of Civil and Environmental Engineering, Colorado School of Mines, Golden, CO 80401, USA *Corresponding author

Abstract

This paper presents a rational procedure to obtain an optimized design for mass timber rocking wall systems utilizing a genetic algorithm (GA) beyond typical displacement-based design metrics for wood buildings. By formulating drift targets and other structural design limit states within an elimination step of the GA optimization process, the method proposed here enables optimization of rocking wall design parameters for an additional enduser criterion beyond satisfying displacement-based seismic design targets. An optimization such as this is difficult to perform using manual trial-and-error approaches. An existing simplified nonlinear time history simulation model (validated through full-scale shake table test data) of a wood rocking wall is employed in this process. The design for an example building in Seattle with a six-story rocking wall is presented using the proposed procedure. The results revealed that the optimization of the mass timber rocking wall lateral system can be achieved in a reasonable time frame using the proposed method. Using the same drift limit objectives, the final designs were found to be different optimization objectives. This indicates a potential to further refine displacement-based design for wood rocking wall systems using computerized tools.

Keywords: Displacement-based design; Genetic algorithm optimization; Mass timber rocking wall; Nonlinear time history analysis.

1 Introduction

1.1 Performance-based seismic design of wood buildings

Performance-based seismic design (PBSD) has been studied by many researchers and applied to a variety of structure types in the past few decades. Specifically for wood-frame buildings, the majority of procedures for PBSD have focused on controlling inter-story drift because it directly correlates to building damage. A typical example of displacement-based design targets is shown in Table 1. Because engineers are encouraged to apply all available techniques and tools to achieve the pre-selected targets, PBSD does not dictate the particular engineering design methodology to be used. The origin of PBSD on wood-framed buildings can be traced back to the time right after the Northridge Earthquake; a large research effort was taken by the Consortium of Universities for Research in Earthquake Engineering (CUREE) and California Institute of Technology (Caltech) (known as CUREE-Caltech Wood-frame Project) to investigate the performance of light-frame wood buildings under earthquake events. This landmark investigation included a series of shaking table tests [1] and recommendations on improved practices in wood building design and construction. Several numerical models of wood-frame buildings were also developed and validated [2, 3, 4]. In the 2000s, an NSF-funded NEESWood Project built on the foundation of existing studies and developed a PBSD philosophy for midrise wood-frame buildings [5]. It was in this philosophy that a displacementbased seismic design procedure was recommended as the main approach [7,8,9]. Additional performance criteria, such as cost, were considered part of the NEESWood efforts and required an iterative trial-and-error process using time history simulations [6,10]. For wood buildings, the premise of a practical PBSD target is closely linked with displacement metrics, such as the example presented in Table 1 (these values represent commonly adopted drift limits for wood buildings). The design process to achieve these targets is mostly manual trial-and-error iterations.

Table 1. Example performance and corresponding seismic hazard levels

Seismic Hazard Levels	Example target performance objectives			
Service Level Earthquake (SLE)	0.5% drift with 50% NP (Non-exceedance Probability)			
Design Basis Earthquake (DBE)	2% drift with 80% NP			

Maximum Considered	4% drift with 70% NP
Earthquake (MCE)	476 drift with 7076 NF

Given a set of performance targets, the engineer can employ any approach deemed appropriate to develop trial designs. The design is considered complete once all design targets are met or exceeded. It is typically not possible to find a design that will meet every target precisely (or closely) at the same time since these performance targets are arbitrarily chosen. This condition will result in one of the performance objectives being the "control" case while others are (sometimes greatly) exceeded. This is inherently unavoidable because the end-user proposing these targets typically does not have enough knowledge about the behavior of the design to propose "compatible" targets among all intensity levels. A more relevant limitation of the existing PBSD procedure is that there is no inherent optimization formulated into the specified requirements. The solution to a given set of performance targets is usually not unique. Among all possible solutions, some will have better characteristics (e.g. costs, serviceability, etc.) than others. The existing methodology for wood-frame building PBSD does not necessarily lead to an optimized solution, nor point to a clear winner among finalists.

This limitation partially originates from the trial-and-error process utilized, which is already labor-intensive to satisfy the drift targets. Further optimization (although it could improve the quality of design) is impractical unless it can be automated via a computerized algorithm. The main objective of this study is to develop a procedure to automate the search for optimized solutions beyond traditional PBSD targets for wood buildings using a mass timber rocking wall lateral system. This was accomplished by applying a genetic algorithm to identify key design parameters of post-tensioned mass timber rocking walls. The following sections detail the approach to incorporate structural design requirements and additional optimization constraints in a standard genetic algorithm searching process. The mass timber rocking wall system was chosen here because of the simplicity of its design parameters. Finally, an example wall design for a realistic building will be presented.

1.2 Mass timber rocking wall system

As interest in mass timber buildings grows globally, there have been considerable efforts around the world to develop the potential for mass timber panel-based lateral force resisting systems. Cross laminated timber (CLT) is a relatively new engineered wood product that is considered a viable option for lateral systems in mass timber buildings. By laminating layers of timber boards in an orthogonal pattern, a solid wood panel is created that can be used for floor or walls. Some research efforts used CLT as a panelized wall system. For example, the Canadian Network for Engineered Wood-Based Building Systems (NEWbuildS) proposed an innovative lateral resisting system with Laminated Strand Lumber (LSL) panels through a series of testing and numerical studies[11]; panelized Cross Laminated Timber (CLT) walls were studied by researchers in Canada and the U.S. [36] [12] [14]. In addition, CLT panels are very similar to pre-cast concrete panels but with less weight and stiffness. Using concepts similar to post-tensioned (PT) concrete rocking walls, developed for high seismic regions [15], PT rocking walls made of CLT have been studied by a number of researchers around the world [13][16]. In its simplest form, a CLT rocking wall can be made with a monolithic panel and vertical PT elements anchored to the foundation to provide a self-centering ability, while utilizing energy dissipation devices (e.g. U-shaped steel plate (UFPs) [17], Resilient Slip Friction (RSF) joints [18], and high-force-to-volume (HF2V) dampers [19]) for energy dissipation. In the U.S. a number of CLT rocking walls have been tested at the component level [20] and in a full-scale building [21]. These experimental studies provided valuable data to develop accurate models for this system, which can be used for dynamic response production. So far, there has not been any prescriptive design approaches developed for CLT rocking walls in the U.S. Thus, all CLT rocking wall designs to this date are performance-based and utilized trialand-error iteration processes. Because a PT rocking wall design configuration can be represented by a relatively small number of key parameters (compared to traditional light-frame wood shear wall system), a rocking wall design can be conveniently "encoded" as a "genetic vector." The simplicity of the design and the ability to assess dynamic response using a numerical model make this system a good candidate to test the idea of automatic optimization PBSD using a genetic algorithm (GA).

1.3 Previous studies of GA used in structure design

Genetic algorithms are a well-developed method for solving both constrained and unconstrained optimization problems through a simulation of biological evolution. The algorithm repeatedly modifies and propagates a population of solutions between different generations. At each generation, the algorithm filters the population based

on certain selection criteria, then randomly uses the filtered population as a parent to produce offspring for the next generation. Over successive generations, the population evolves towards an optimal solution. The advantages of a GA include its implementation simplicity, robustness against changes in circumstances, and flexibility [22]. Previous studies have shown that these algorithms can be an appropriate tool for many engineering design solutions [23]. GAs have been used in PBSD of structures with specific optimization constraints. For example, Liu et al. [24, 25] set material usage and construction expenses as the optimization constraints to seek design solutions that maximize efficiency. Foley et al. [26] provided a probabilistic performance-based seismic design methodology for single-story and multi-story steel moment-resisting frames to achieve multiple-objective optimization targets. Sung et al. [27] used a GA optimization solver to minimize construction cost for performance-based seismic design for reinforced concrete bridge piers. There has not been any notable study which combines particular optimization criteria with traditional PBSD drift criteria, or any study that incorporates the GA application in mass timber building design.

2 Formulating PBSD of rocking wall as a GA problem

In this study, we aim to develop a GA process which allows mass timber rocking wall designs to achieve (1) existing PBSD drift targets, and (2) a given additional optimization constraint. For example, a rocking wall design will satisfy drift limits set at different intensity levels with a needed non-exceedance probability AND be the solution that requires the least amount of material. This process is conducted in the following steps:

- 1) Parameterizing the design space. For a specific design condition, the architectural configuration of the building will be given, this includes the number of stories (N), story heights $(H_1 H_n)$, and tributary seismic mass for each rocking wall at each story $(M_1 M_n)$. Then the genetic sequence of the rocking wall design can be constructed using the following design parameters: aspect ratio of the rocking panel (height to width ratio), amount of Post-tensioned steel area, initial Post-tension force, the thickness of the rocking panel, initial stiffness of energy dissipation device (U-shaped Flexural Plates (UFPs) are used here as an example), and yield deformation of the UFPs. The designer can determine a range of these parameters based on experience and architectural constraints. Then the GA can be set up to generate the population.
- 2) Define a design target with both traditional PBSD drift requirements and optimization criteria. In this study, an additional optimization criterion is added to the traditional PBSD targets to provide the constraint needed to identify the optimal design beyond traditional drift targets. This optimized PBSD design target simply includes traditional targets with the desired probability of exceedance plus one additional optimization criteria. For example, an optimized PBSD target may include:

Maximum inter-story drift at SLE <0.5% with 50% NP (Non-exceedance Probability) Maximum inter-story drift at DBE <2% with 80% NP Maximum inter-story drift at MCE <4% with 70% NP And the additional optimization constraint: minimum total cost of rocking wall material

- 3) Performance assessment under prescribed hazard levels. This step is no different than the traditional simulation-based PBSD processes. The difference here is a population of different designs generated by the GA will be used in an automated simulation process to assess their performance. For every simulation, maximum inter-story drift and the optimization parameter (e.g. cost) will be produced. A suite of earthquake ground motions will be pre-selected and scaled to desired hazard levels to represent seismic input uncertainty. The simulated results from the individual earthquake input will be treated as a sample from the response distribution. Due to a large number of simulations needed, a highly computationally efficient model is necessary to make this process practical.
- 4) GA elimination and generation. Different from the traditional GA process that focuses mostly on optimization through a particular fitness function, the structural design using the GA will include two distinct elimination steps before checking the fitness function. The first elimination step is used to ensure that the population will achieve PBSD targets by conducting a pass-fail check. The logic "AND" operation was used to conduct this check to ensure all traditional PBSD targets were met or exceeded at the same time. The GA program can be set up to continuously generate random designs until enough gene samples can "pass" the elimination. After the first round of elimination (when the desired size of the population is obtained), individual designs within the population will go through a second elimination procedure, which

is based on structural design limit state checks (e.g. material strength, component capacity). After this elimination process, only designs meeting all displacement and structural limit states will remain. The limit states for wood rocking walls that were checked in this study include the CLT compression strain check, the PT initial stress check, and the PT restoration limit check. This list can be expanded to other design requirements that the user deems necessary. After the elimination steps, a standard optimization GA with the fitness function, designed to reflect the optimization criteria, is followed to advance the population into the next generation. Two fitness functions have been used in this study. The first is material expenses of wood panel and steel, the second is average peak roof acceleration under DBE earthquakes.

This four-component design process is illustrated in Fig. 1. A design example is presented in the next section to demonstrate the implementation of this process.

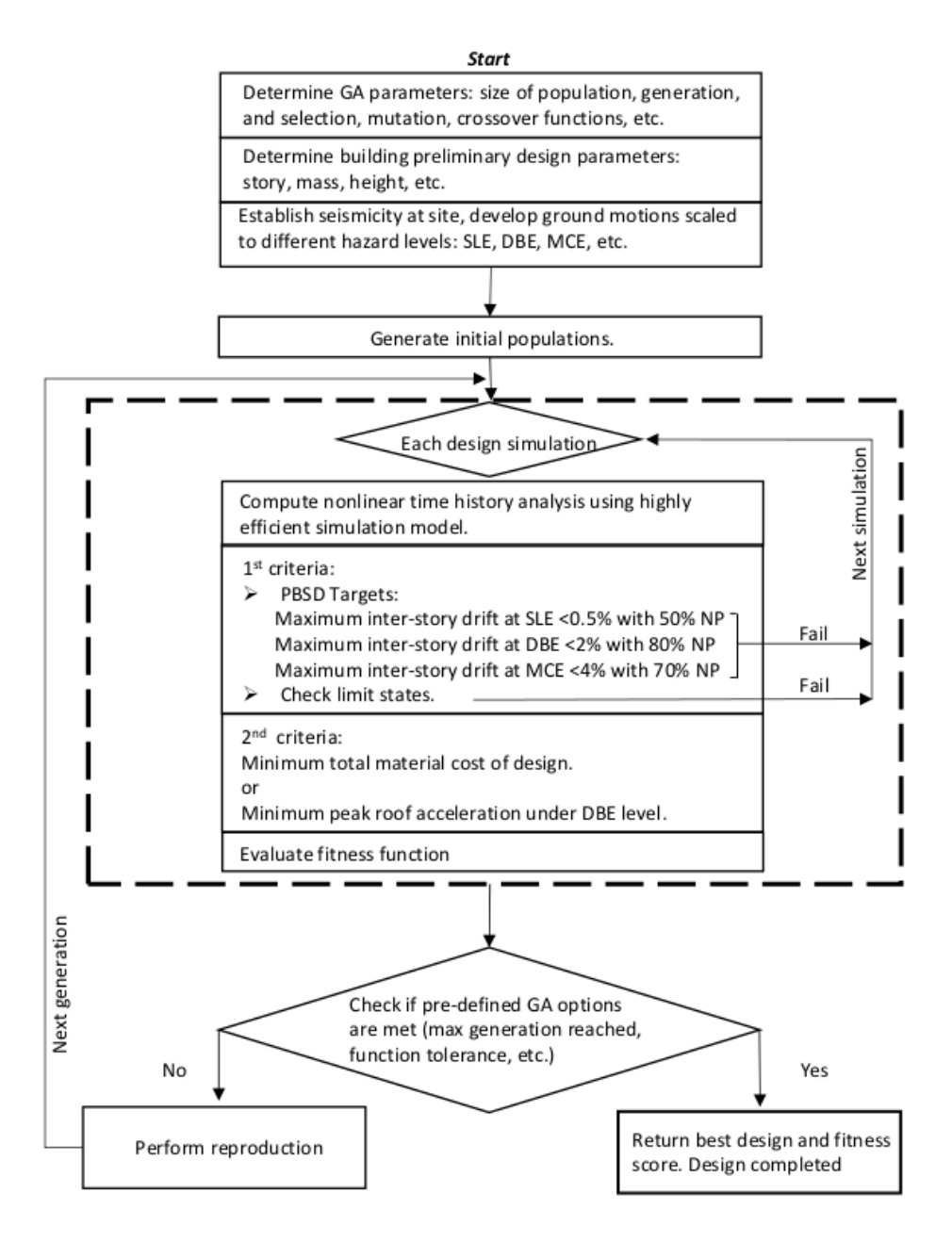


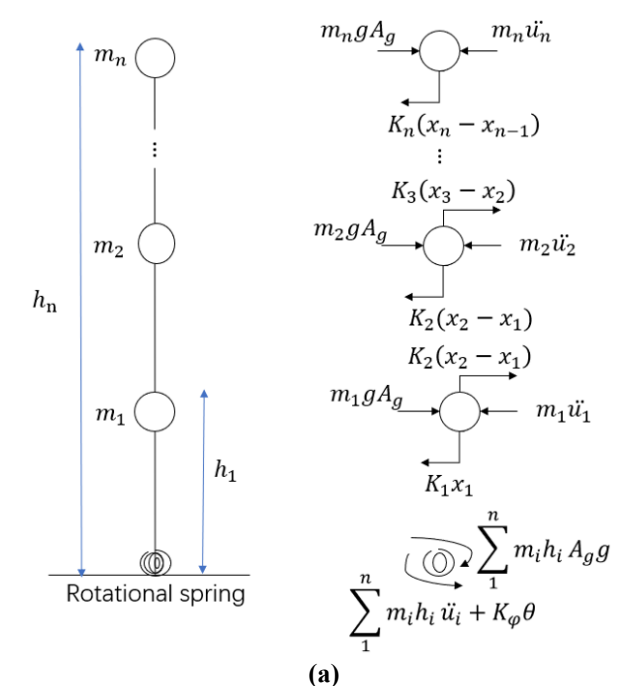
Fig. 1, Design optimization process flowchart

3 Simplified numerical model

 A key component that made GA optimization possible is a simplified numerical model that (1) can simulate the seismic response of the rocking wall system with a reasonable level of accuracy, (2) has high computational efficiency, and (3) can be automatically constructed using the limited design parameters included in the gene vector. A simplified model shown in Fig. 2 was used in this study to conduct a time history response simulation. This simplified model can be used to model multi-story buildings with balloon-framed rocking walls as the lateral system. Building diaphragms and the distributed seismic mass can be modeled as a lumped mass at each story level. The dynamic force equilibrium can be established through a system of equations based on the dynamic force balance at each story, as shown in Fig. 2 (a). The rocking walls are modeled as linear beam elements with a non-linear rotational spring at the base. The parameters for the linear beam elements are derived based on the dimensions of the CLT rocking panel. The parameters for the nonlinear rotational spring are calculated based on the location and size of the PT and energy dissipation elements. The instantaneous stiffness of the rotational spring can be derived based on the principle of virtual work as:

$$K_{\varphi} = \sum K_{pt} y^2 + \sum K_{UFP} b^2 \tag{1}$$

where K_{φ} is the rotational stiffness, K_{pt} is the stiffness of PT bar, K_{UFP} is the stiffness of UFPs, y is the distance from the location of each PT bar to the edge of each CLT panel, and b is the width of the CLT rocking panel. The performance of nonlinear hysteresis of the rotational spring for a typical CLT rocking wall design is shown in Fig. 2 (b). Typically, the hysteresis behavior will have 4 phases: at low ground accelerations and low spring rotations (Phase 1 in Fig. 2 (b)), the system has a high level of stiffness because the post-tensioned force fixes the wall to the foundation. Once the external lateral force is sufficient to overcome the initial compressive stress at the base of the wall, the post-tensioned bars begin to elongate, and the wall panel begins to uplift. The point at which uplift begins is referred to as the decompression point. During Phase 2, the UFPs and the couple between the PT bars act against the compression force at the base of the wall, generating a resisting moment while all materials remain elastic. In Phase 3, the rotation becomes large enough for the UFPs to begin yielding, and in Phase 4, PT bars begin yielding, resulting in a decrease in rotational stiffness. It should be noted that the PT force will be lost if PT bars start to experience yielding and the system may not be able to re-center by itself. This characteristic is not reflected in this simplified model because the yielding of a multi-story long PT bar requires large deformation of the building thus is rare in real designs.



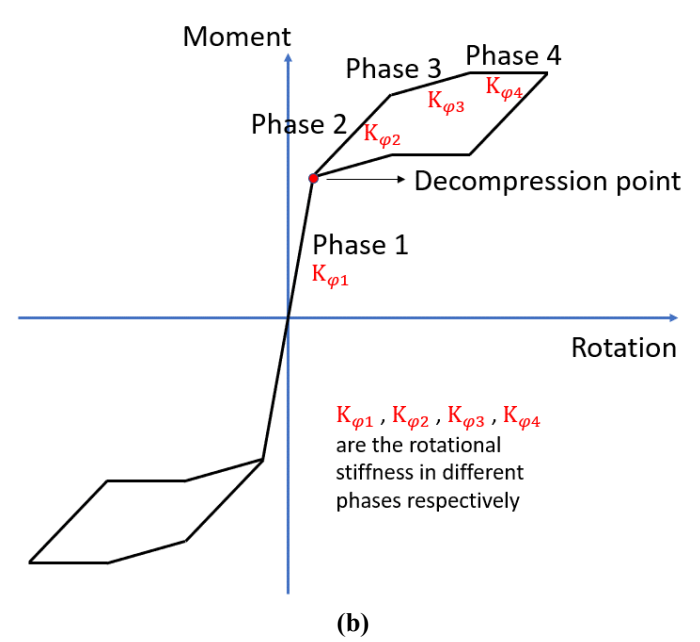


Fig. 2, (a) DOF of rocking wall systems, (b) nonlinear hysteresis of rotational spring

This simplified numerical model was validated using data from a series of full-scale shake table tests from a two-story mass timber building [28]. For the brevity of this paper, the comparison of the displacement time history for the roof between the test results and the numerical simulation at different intensity levels is shown in Figure 3. The comparison showed reasonable agreement between the numerical model and the test data at all intensity levels.

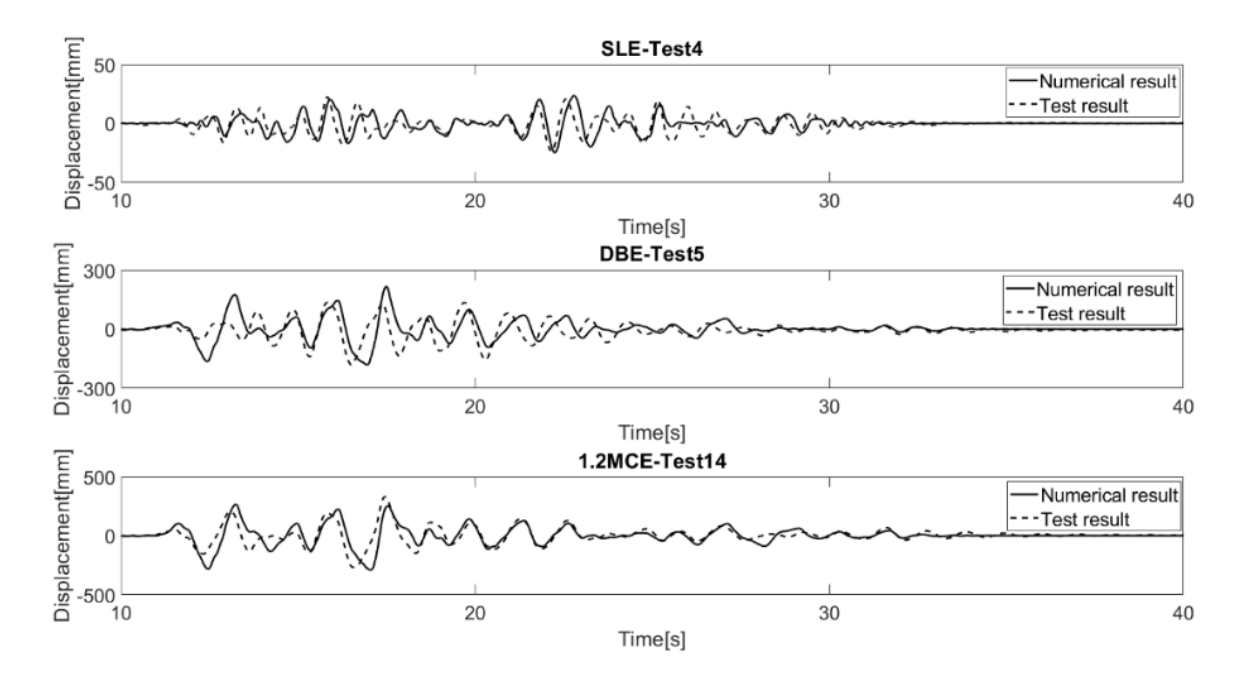


Fig. 3, Comparison of time history responses at the roof level

The numerical model was implemented in Matlab to automatically conduct a simulation with multiple ground motion records and develop a pass-fail probability based on simulated responses and corresponding performance targets. Incorporation of this pass/fail criteria in the GA was accomplished by assigning an infinite fitness score to the samples that failed to satisfy the design requirements (the fitness score is to be minimized in this case). This will ensure that the designs that failed the structural design and drift performance targets will be eliminated automatically

by the GA. The additional optimization criteria can essentially be anything the user wants, as long as the objective can be calculated based on the numerical simulation results for each design. In the following section, we will demonstrate the application of this optimization process by applying two different optimization criteria to the same set of traditional PBSD drift targets. It will be shown that the proposed GA process does result in different designs that are acceptable for traditional drift targets but have distinctive traits.

4 Design examples

In order to demonstrate the proposed design procedure, an example building will be designed with two different optimization criteria. The first criterion is to achieve minimum material costs for the rocking wall system, which is simplified as the volume of the rocking wall panels and the amount of steel material used (more realistic cost estimation including construction costs were not considered in this illustrative example). The second criterion aims to achieve the lowest overall floor acceleration during a design level earthquake (DBE). The building was a six-story office structure located in Seattle, with risk category 2 and site class C. The Design response spectrum is shown below in Figure 4 (ASCE 7-16). The design response spectrum value at the estimated building period was used to scale the ground motion suite that contains 10 recorded ground motions. The approximate fundamental period of the building based on ASCE7-16 (Equation (2)) is 0.75s, with the design spectrum acceleration equal to 0.64g.

$$T_a = C_t h_n^{\ x} \tag{2}$$

 C_t and x are empirical data parameters obtained from ASCE 7-16 table 12.8-2. h_n is the building height.

The scaling of the ground motion suite was conducted based on this target spectral acceleration point for the DBE level. The scale factors for SLE and MCE level earthquakes are simply taken as 0.5 and 1.5 from the DBE level magnitude. Scale factors for the DBE level can be found in Table 3. While there are a variety of methods to select and scale Ground Motion (GM) inputs, GM records from the CUREE Woodframe project [29] were used with a simple scaling method since the example is only for illustrative purposes of the proposed procedure. More advanced, site-specific selections and scalings should be adopted for realistic projects.

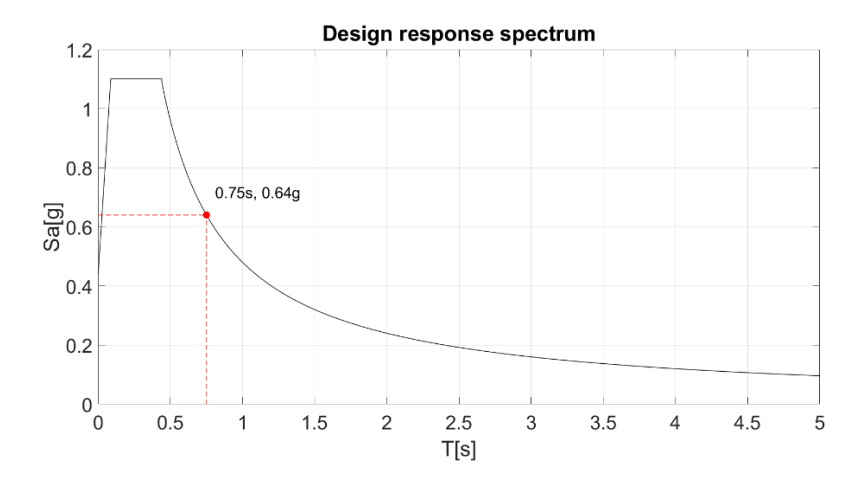


Fig. 4, Design response spectrum

The architectural design of the building was based on the size of realistic urban plot development with 61.0m (200') by 30.5m (100'). The building was assumed to be a mixed-use commercial, office, and residential construction. Each of the floors was assumed to have a total dead load of 3.35 kN/m² (70 psf), this includes the self-weight of the CLT floors with the additional weight of the permanent building components. The floor plan of the typical floor is shown in Fig. 5. The location of the rocking walls was pre-selected based on the architectural floor layout and design experience.

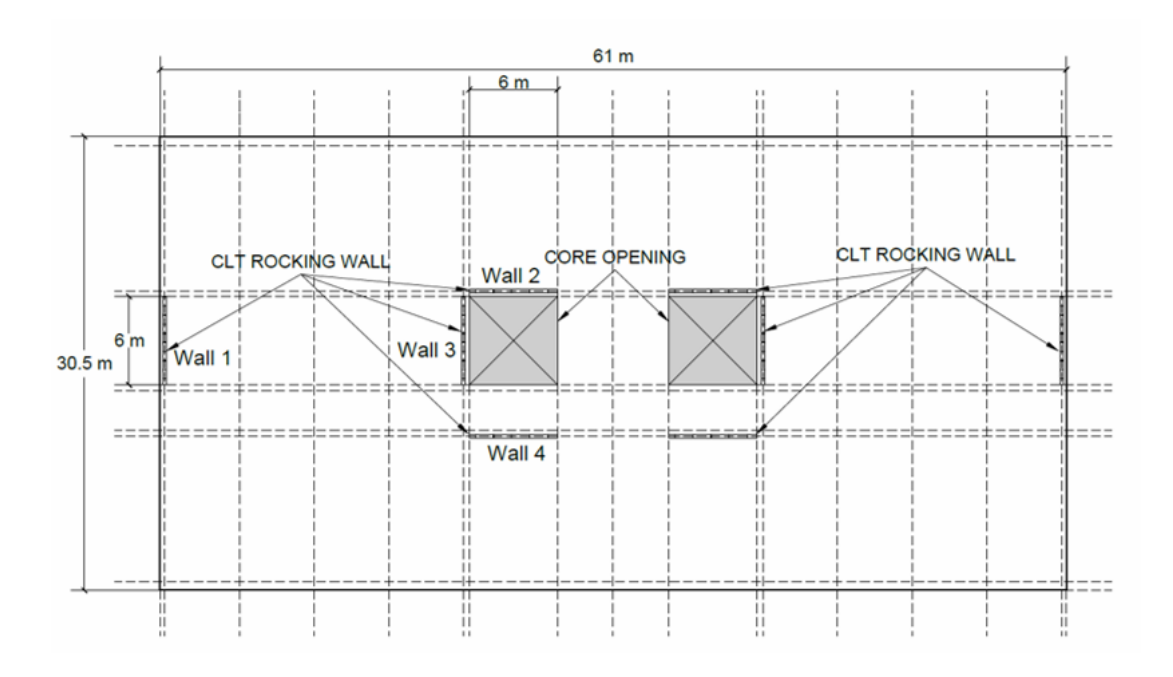


Fig. 5, Floor plan

The height of the first story is 6.1m (20ft) with the remaining stories having a height of 3.7m (12 ft). The building has eight CLT rocking walls, each with a length of approximately 6 m (19.5ft) as shown in Fig. 5. But the actual length of the wall will be determined later through the automated design process. Based on these building parameters and layout shown above, the tributary mass on each of the walls can be calculated. Due to the symmetric nature of the building, the tributary load calculations, shown below, only feature four of the eight walls, as labeled in Fig. 5.

- Wall 1:

- o Tributary Area: 3790.4 m² (40800 ft²)
- o Tributary Mass: 76224.7 kN (17136 kips)
- Wall 2:
 - o Tributary Area: 5253.5 m² (56549 ft²)
 - o Tributary Load: 105714.2 kN (23766 kips)
- Wall 3:
 - o Tributary Area: 6934.0 m² (74637 ft²)
 - o Tributary Load: 139438.4 kN (31347 kips)
- Wall 4:
 - o Tributary Area: 5470.9 m² (58889 ft²)
 - o Tributary Load: 110018.8 kN (24733 kips)

In this design, we assumed that all walls use CLT panels that conform to the PRG320 material standards [30]. The key mechanical and physical properties of the CLT panel and the steel include: the elastic modulus of CLT (E_{CLT} =12.41 Gpa (1800 ksi)), the elastic modulus of steel (E_{steel} =199.95 Gpa (29000 ksi)), and the yielding stress of PT steel (ε_y = 724 Mpa (105 ksi)). With the material and building parameters are given (set as constants) above, the design process focused on optimizing the variables listed in Table 2 through the proposed GA process. Table 2 also shows the realistic ranges for these variables to use as boundaries. These boundaries were determined based on the practical constraints of the materials and constructability. Buildings with the systems and components outside of these boundaries are unlikely to get built in real circumstances. Setting these boundaries is an essential step for a realistic design using the GA approach.

Table 2, Boundary condition of design variables

	Aspect ratio	Amount of PT[cm ²]	PT initial forces[kN]	Wall thickness[cm]	$K_{UFP}[kN/mm]$
Lower bound	1:1	32.3	233.5	11.4	1.2
Upper bound	10:1	322.6	11676.6	63.5	383.2

The aspect ratio listed is the ratio of the height to the width of the rocking wall panel. Any value higher than 10:1 would likely make the lateral system too flexible to satisfy serviceability requirements on stiffness and vibration. The amount of PT is controlled by the total cross-sectional area of the post-tensioned bars that can be realistically installed. The wall thickness range is estimated from that of a typical 3-ply CLT panel, up to that of a set of double 11-ply panels used side by side (with PT going through the center), K_{UFP} is the initial stiffness of UFPs, calculated based on the equation below [31].

$$K_{UFP} = \frac{(16*E*b_u)}{27\pi} \left(\frac{t_u}{D_u}\right)^3 \tag{3}$$

Where this stiffness is determined by two factors, the width of UFP (b_u) , which is typically available in the range of [10.2 cm (4in) 25.4 cm (10in)], and geometric ratio $(\frac{t_u}{D_u})$, which it is typically selected within a range of $[0.04 \ 0.2]$

As it was mentioned earlier, a suite of ten earthquakes GM records from the CUREE project were used in this example, the detailed information of the records is shown in Table 3 (with the original record PGA values and the scale factor for the DBE level hazard). The response spectrum of the 10 ground motions scaled to the DBE level is shown in Figure 6.

Table 3, Information of the ten earthquake ground motion records used

EQ	Year	Record ID	Earthquake event	Station	PGA(g)	Scale factor (DBE)
1	1992	LD92dsp	Landers	Desert Hot Spring	0.154	2.436
2	1992	LD92yer	Landers	Yermo Fire Station	0.152	2.481
3	1989	LP89cap	Loma Prieta	Capitola	0.529	0.841
4	1989	LP89g03	Loma Prieta	Gilroy Array #3	0.555	1.298
5	1989	LP89g04	Loma Prieta	Gilroy Array #4	0.417	1.834
6	1989	LP89gmr	Loma Prieta	Gilroy Array #7	0.226	2.072
7	1989	LP89hda	Loma Prieta	Hollister Diff. Array	0.279	1.051
8	1989	LP89wvc	Loma Prieta	Saratoga – W Valley Coll.	0.332	0.926
9	1994	NR94mul	Northridge	Beverly Hills 14145 mulhol	0.416	0.752
10	1994	NR94cnp	Northridge	Canoga Park – Topanga Can	0.356	1.144

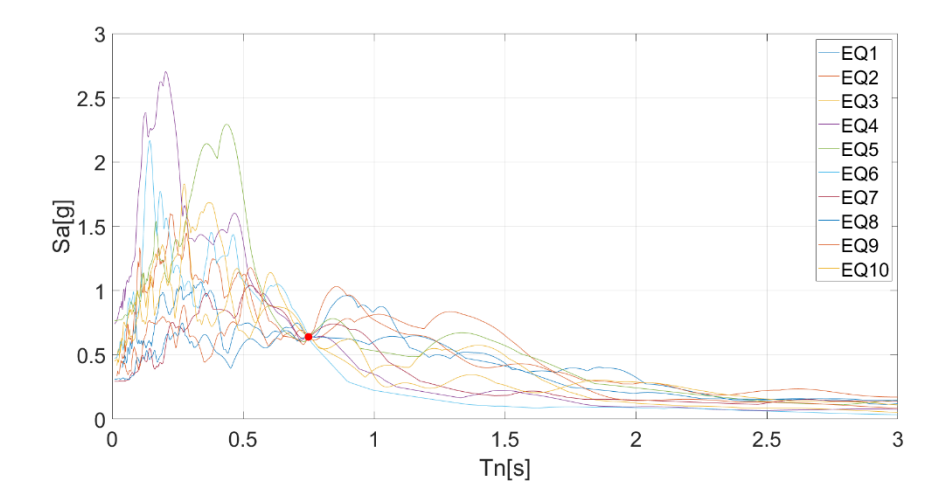


Fig. 6, Scaled response spectrum for DBE level ground motions

4.1 Design objectives

 Design objectives used in this example building include the traditional displacement-based design inter-story drift limits listed below for the three different hazard levels:

- Maximum inter-story drift at SLE <0.5% with 50% non-exceedance probability (NP)
- Maximum inter-story drift at DBE <2% with 50% NP
- Maximum inter-story drift at MCE <4% with 50% NP

In addition, two different optimization criteria were used in this example to illustrate the effect of the proposed process. These different optimization criteria will demonstrate that different designs will be generated with identical drift requirements. The first optimization criterion is to achieve minimal total cost for materials (wood and steel); the second criterion seeks to minimize the peak acceleration experienced on the roof under DBE level earthquakes (the average peak acceleration from all 10 DBE ground motions was used as the target metric). The designs resulting from these two criteria are termed hereafter as Design 1 (cost minimization) and Design 2 (acceleration minimization), respectively.

Aside from system-level drift requirements, structural design of rocking walls may require additional mechanical limit state checks. In this example, three additional limit states were included in the GA elimination process, namely the CLT panel compression strain limit, PT initial stress limit, and PT restoration limit. The CLT compression strain check was designed to prevent crushing at the decompression corners of the CLT panel based on the following equation:

$$\frac{\varepsilon_{wood}}{\varnothing \varepsilon_u} \le 1.0 \tag{4}$$

where ε_{wood} is the compression strain of wood, \emptyset is the strength reduction factor by NDS [32], and ε_u is the ultimate strain of wood.

The PT initial stress check applies an empirical limit to keep the initial PT force lower than 50% of the yielding force of the PT bars:

$$\frac{F_{ini}}{F_V} \le 0.5 \tag{5}$$

Finally, the PT restoration limit check was done to ensure there is enough restoring force in the PT system to overcome the yielding demand of the UFP elements, so that the wall can still re-center when UFPs reach yielding:

$$K_{UFP} * d_{\nu} < 0.5 * F_{\nu} \tag{6}$$

It is worth pointing out that currently there is no prescriptive design method for mass timber rocking walls in the U.S. codes. There is an on-going effort aiming at developing seismic design approaches for post-tensioned mass timber rocking wall systems [37]. Thus, the design checks listed here may not be comprehensive. For demonstrative purposes, the three additional design checks applied here illustrate how the additional pass/fail type design criteria can be incorporated in the proposed process.

4.2 Optimization and results

In the general GA process, one can set up an automatic termination trigger to detect convergence so that the search process will be more "intelligent" and stops automatically. In this example, we elect to not implement such a trigger, but simply let the GA run 30 generations (this number was arbitrarily chosen based on observation of the convergence trend) to ensure convergence and to show that the convergence for wood rocking walls can occur relatively fast. It was shown that both designs converged to a local optimization point in just a few generations and remained there for the rest of the iterations. There are 500 designs in each generation.

Initially, the population was generated by creating a random initial population with design parameters sampled from the uniform distributions within the ranges shown in Table 2. This population was subjected to the design requirement checks described earlier to filter out the failed designs. This process was repeated until the desired number of samples was reached (500 in this case). Then the next generation was produced by combining a stochastic uniform selection function, a Gaussian mutation function, and a scattered crossover function [33]. Based on the given simulation parameters, a total of 900,000 nonlinear time history analysis simulations were conducted for Design 1 and 2. Using this model, it takes about 0.26 seconds to simulate the response of the example building under a 35-second earthquake record on a typical desktop computer (Intel i7-7700 CPU @ 3.60 GHz and 16GB RAM). Fig. 7 shows the change in fitness function values for the two design cases over the 30 generations. One can see the change in the fitness function value for Design 1 (cost) seemed to be more significant than that of Design 2 (roof acceleration). This is expected because it is relatively harder to reduce floor accelerations (compared to cost reduction) within the available system parameter space when the height and mass of the building and the input seismic intensity are given. For both cases, the designs converge to the final solution after about 5 generations, highlighting the efficiency of the algorithm. Figure 8 further illustrates the change of the actual design parameters from different generations. The design parameters shown in Figure 8 came from the sample which had the best fitness function value in each generation. According to Figure 8, for Design 1, the aspect ratio, amount of PT, PT initial forces, and wall thickness reach their final solution quickly, the UFP stiffness hops around and then stable at the end. For Design 2, the amount of PT, and PT initial forces have the same pattern as Design 1, the aspect ratio, wall thickness, and the UFP stiffness hops around a bit and then reach their final solution.

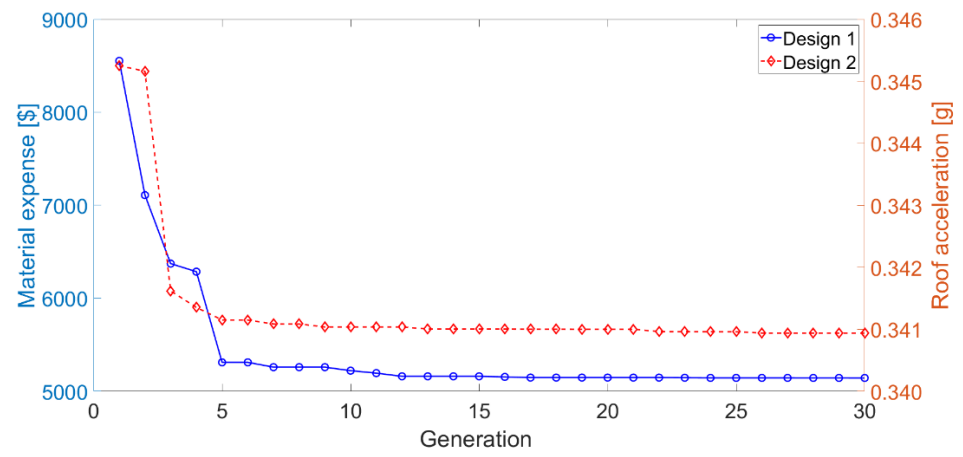


Fig. 7, Fitness function change during GA

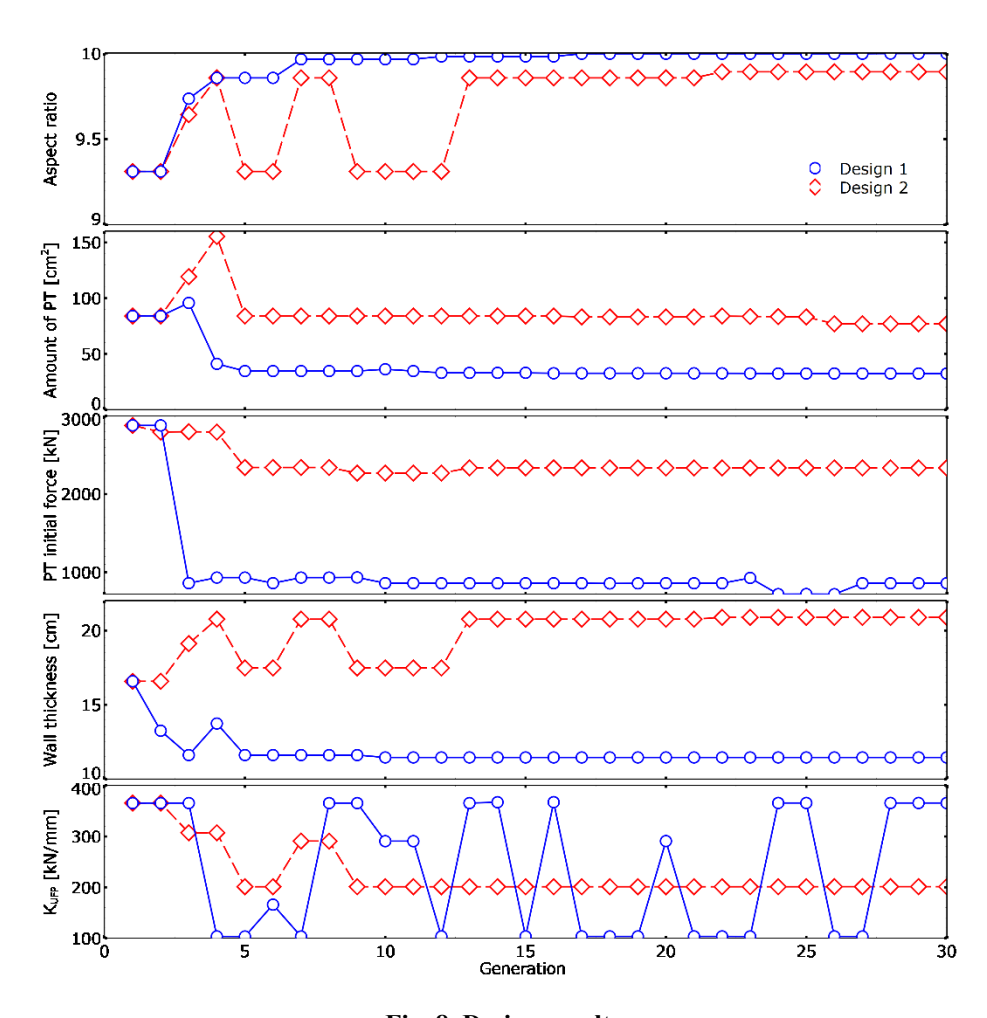
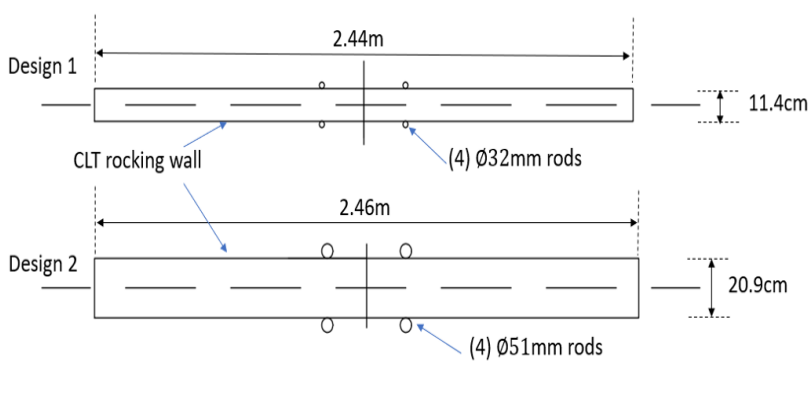
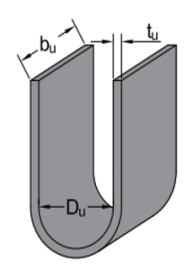


Fig. 8, Design results

Based on the GA process, Design 1 was finalized with a panel thickness of 11.4 cm, 4 Ø32mm (1-1/4in) rods, 12 UFPs with a width of 102mm (4in), and a panel length of 2.44m (the height of the rocking wall is the same as the building height). Design 2 utilized a much thicker 20.9 cm panel, 4 Ø51mm (2in) rods, 5 UFPs with a width of 127mm (5in), and a panel length of 2.46m. The physical dimensions of these two designs are shown in Fig. 9.





Design 1: UFP number : 12 tu/du=0.2 tu=19mm (0.75in) Du=95mm (3.75in) bu=102mm (4in)

Design 2: UFP number : 5 tu/du=0.2 tu=19mm (0.75in) Du=95mm (3.75in) bu=127mm (5in)

(b) Fig. 9, (a) Configuration of Design 1 and Design 2, (b) UFP details

As mentioned before, Design 1 is based on the total material cost of the rocking wall itself. The final design is expected to have the lowest material cost among all possible designs and also pass all traditional PBSD drift targets. In this example, we assume the average production cost of CLT to be \$678.45 per cubic meter [34], and the average production cost of carbon steel as \$6712.64 per cubic meter [35]. Such values do not reflect construction costs or the scale of production but serve as a pure thought experiment to help illustrate the optimization outcome. The total material cost of Design 1 was calculated to be \$5,144. This design (which is not optimized for floor acceleration) produced an average peak roof acceleration of 0.425g at the DBE level. The probability of the non-exceedance level of the inter-story drift criterion from this design were 60%, 80%, and 90% under SLE, DBE, and MCE, respectively, all exceeding the NP target of PBSD. It is common to see PBSD satisfying a control case (SLE in this example) while greatly exceeding other cases in terms of NP [6].

Design 2, which was optimized for average peak roof accelerations at the DBE level, lowered the average roof acceleration to 0.341g. It also surpassed all traditional PBSD targets with NP levels of 50%, 80%, and 90% under SLE, DBE, and MCE, respectively. The total material cost of Design 2 is \$9,838, which is significantly higher than that of Design 1. The comparison is based on limited cost data but illustrates a drastic relative difference which was achieved by introducing an additional cost constraint. It should be mentioned that in this example, Design 1 only lowers the material cost. Installation costs and other factors are not considered. This design method can provide the optimized design solutions based on users' objectives; users can make their own decision based on their engineering judgment combined with this method. Further refinement can be considered in this method, such as a comprehensive estimation of damage relative not only drift but also story acceleration, and strictly cost estimation.

5 Conclusion

This study explored the possibility of further optimizing displacement-based seismic design by introducing additional design criteria that can be implemented automatically using a Genetic Algorithm. An automated procedure was developed to achieve an optimized design for post-tensioned mass timber rocking wall systems while satisfying other structural and drift requirements. A two-step elimination process was introduced before the fitness function evaluation in order to produce structurally sound and realistic rocking wall designs. The evaluation of the fitness function for individual designs was conducted using a simplified numerical model for wood rocking walls which has been validated through large scale shake table tests. The design example for a six-story building in Seattle illustrated the sensitivity of the final design given different optimization criteria. The results confirmed that it is practical to obtain optimized PBSD of a mass timber rocking wall lateral system using the proposed method.

While this study focused mainly on the integration of a GA with PBSD, the actual GA program used in the example of this study is not optimized for this application. This study was mainly focused on demonstrating the viability of the proposed approach using a very basic GA configuration. As the market of mass timber grows, more design data will be available for researchers to advance this proposed approach and further optimize the incorporated algorithm. Due to the simplicity and flexibility of the GA, users will have a wide range of freedoms to customize the algorithm to better achieve an optimal solution that depends on their unique priorities and constraints. In order to make this

procedure more practical and efficient, additional refinement on the GA algorithm and termination triggers should be investigated to make the process "smarter". In addition, consideration of more complicated performance targets (e.g. damage and cost) can be implemented through the integration of fragilities of nonstructural components and other features of the building systems in the GA process.

ACKNOWLEDGMENTS

This research project is supported by the National Science Foundation through grant CMMI 1636164 and U.S. Forest Services through the Wood Innovations Grant program. The financial support from the sponsors is greatly appreciated. The opinions and conclusions presented in this article are of the authors themselves but not the sponsors. The authors also would like to acknowledge Jonathan Heppner and Thomas Robinson at LEVER Architecture for providing the example building floor plan used in this study.

REFERENCES

- [1] Fischer, D., Filiatrault, A., Folz, B., Uang, C. M., Seible, F., "Shake Table Tests of a Two-Story Woodframe House," CUREE Publication No. W-06, CUREE-Caltech Woodframe Project, 2001.
- [2] Folz, B., and Filiatrault, A., Seismic analysis of woodframe structures. I: Model formulation. Journal of Structural Engineering, 130(9): 1353–1360, 2004a.
- [3] Folz, B., and Filiatrault, A., Seismic analysis of woodframe structures. II: Model implementation and verification. Journal of Structural Engineering, 130(9): 1426–1434, 2004b
- [4] He, M., Lam, F., Foschi, R. O., Modeling Three-Dimensional Timber Light-Frame Buildings. Journal of Structural Engineering, 127(8): 901-913, 2001.
- [5] van de Lindt, J. W., Rosowsky, D. V., Pang, W., Pei, S., Performance-Based Seismic Design of Midrise Woodframe Buildings. Journal of Structural Engineering, 139(8): 1294-1302, 2013.
- [6] Pei, Shiling, and John W. van de Lindt. "Systematic seismic design for manageable loss in wood-framed buildings." Earthquake spectra 25, no. 4 (2009): 851-868.
- [7] Pang, W., Rosowsky, D. V., Pei, S., van de Lindt, J. W., Simplified Direct Displacement Design of Six-Story Woodframe Building and Pretest Seismic Performance Assessment. Journal of Structural Engineering 2010; 136(7): 813-825.
- [8] Pang, W., Rosowsky, D. V., Direct Displacement Procedure for Performance-Based Seismic Design of Mid-Ris Wood-Framed Structures. Earthquake Spectra, Vol. 25, No. 3, 583-605, 2009.
- [9] Wang, Y., Rosowsky, D. V., Pang, W., Performance-Based Procedure for Direct Displacement Design of Engineered Wood-Frame Structures. Journal of Structural Engineering, 136(8): 978-988, 2010.
- [10] Rosowsky, D. V., Ellingwood, B. R., Performance-Based Engineering of Wood Frame Housing: Fragility Analysis Methodology. Journal of Structural Engineering 2002; 128(1): 32-38.
- [11] Chen, Z., Chui, Y. H., Lateral Load-Resisting System Using Mass Timber Panel for High-Rise Buildings. Frontiers in Built Environment, Vol. 3, 40, 2017.
- [12] Popovski, M., Schneider, J., Schweinsteiger, M., Lateral Load Resistance of Cross-Laminated Wood Panels.
 World Conference on Timber Engineering, Riva del Garda, Italy, 2010.
- [13] Moroder, D., Smith, T., Dunbar, A., Pampanin, S., Buchanan, A., Seismic Testing of Post-Tensioned Pre-Lam
 Core Walls Using Cross Laminated Timber. Engineering Structures, 167 639-654, 2018.

- [14] Reynolds, T., Foster, R., Bregulla, J., Chang, W. S., Harris, R., Ramage, M., Lateral-Load Resistance of Cross-Laminated Timber Shear Walls. Journal of Structural Engineering, 143(12): 06017006, 2017.
- [15] Erkmen, B., Schultz, A. E., Self Centering Behavior of Unbonded Precast Concrete Shear Walls. Earthquake
 Resistant Engineering Structures 2007.
- [16] Ganey, R., Berman, J. W., Akbas, T., Loftus, S., Dolan, J. D., Sause, R., Ricles, J., Pei, S., van de Lindt, J. W.,
 Blomgren, H. Experimental Investigation of Self-Centering Cross-Laminated Timber Walls. Journal of Structural
 Engineering 2017;143(10): 04017135.
- [17] Sarti, F., Palermo, A., Pampanin, S., Design Charts and Simplified Procedures for Post-Tensioned Seismic
 Resistant Timber Walls. World Conference on Timber Engineering, Auckland, New Zealand, 2012.

- [18] Hashemi, A., Zarnani, P., Masoudnia, R., Quenneville, P., Experimental Testing of Rocking Cross-Laminated Timber Walls with Resilient Slip Friction Joints. Journal of Structural Engineering 2018; 144(1): 04017180.
- [19] Wrzesniak, D., Rodgers, G. W., Fragiacomo, M., Chase, J. G., Experimental testing of damage-resistant rocking glulam walls with lead extrusion dampers. Construction and Building Materials, 102 1145-1153, 2016.
- [20] Akbas, T., Sause, R., Ricles, J. M., Ganey, R., Berman, J. W., Loftus, W., Dolan, J. D., Pei, S., van de Lindt, J.
 W., Blomgren, H., Analytical and Experimental Lateral-Load Response of Self-Centering Post-tensioned CLT
 Walls. Journal of Structural engineering 2017; 143(6): 04017019.
 - [21] Pei, S., van de Lindt, J. W., Barbosa, A. R., Berman, J. W., McDonnell, E., Dolan, J. D., Blomgren, H., Zimmerman, R. B., Huang, D., Wichman, S. W., Experimental Seismic Response of a Resilient 2-Story Mass-Timber Building with Post-Tensioned Rocking Walls. Journal of Structural Engineering 2019;145(11): 04019120.
 - [22] Sivanandam, S. N., Deepa, S. N., Introduction to Genetic Algorithms. Springer 2008; ISBN: 9783540731894.
 - [23] Jenkins, W. M., Towards Structural Optimization via the Genetic Algorithm. Computers & Structures 1991; 40(5): 1321-1327.
 - [24] Liu, M., Burns, S. A., Wen, Y. K., Multiobjective optimization for performance-based seismic design of steel moment frame structures. Earthquake Engineering and Structural Dynamics 2005; 34:289-306.
 - [25] Liu, M., Burns, S. A., Wen, Y. K., Optimal seismic design of steel frame buildings based on life cycle cost considerations. Earthquake Engineering and Structural Dynamics 2003; 32: 1313-1332.
 - [26] Foley, C. M., Pezeshk, S., Alimoradi, A., Probabilistic Performance-Based Optimal Design of Steel Moment-Resisting Frames. 1: Formulation. Journal of Structural Engineering 2007; 133(6): 757-766.
 - [27] Sung, Yu-Chi, Su, Chin-Kuo, Fuzzy genetic optimization on performance-based seismic design of reinforced concrete bridge piers with single-column type. Optimization and Engineering 2010; 11: 471-496.
 - [28] Pei, S., Huang, D., Berman, J. W., Wichman, S. W., Simplified Dynamic Model For Post-Tensioned Cross Laminated Timber Rocking Walls, Earthquake Engineering and Structural Dynamics 2019, submitted.
- [29] Krawinkler, H., Parisi, F., Ibarra, L., Ayoub, A., and Medina, R., Development of testing protocol for wood frame structures." CUREE Publication No. W-02, Consortium of Universities for Research in Earthquake
 Engineering, Richmond, Calif. 2000.
 - [30] American National Standard Institute (ANSI/APA PRG), Standard for Performance-Rated Cross-Laminated Timber, 2019.

- [31] Baird, A., Smith, T., Palermo, A., Pampanin, S., Experimental and numerical Study of U-shaped Flexural
 Plated (UFP) dissipators. NZSEE Conference, Auckland, New Zealand, 2014.
- [32] American Wood Council, National Design Specification for Wood Construction, 2018 Edition.
- 575 [33] Chipperfield, A. J., Fleming, P. J., The Matlab Genetic Algorithm Toolbox, IEE Colloquium on Applied 576 Control Techniques Using Matlab, Digest No. 1995/014, 26/01/95.
- 578 [34] Karacabeyli, E., Douglas, B. CLT handbook. U. S. Edition, 2013. 579

- 580 [35] World Steel Prices, Global Composite Steel Price and Index (US\$/tonne), From https://worldsteelprices.com/
 581
- [36] van de Lindt, J. W., Furley, J., Amini, M. O., Pei, S., Tamagnone, G., Barbosa, A. R., Rammer, D., Line, P.,
 Fragiacomo, M., Popovski, M., Experimental seismic behavior of a two-story CLT platform building. Engineering
 Structures, 183 408-422, 2019.
- [37] Pei, S., Dolan J., Zimmerman R.B., McDonnell E., Busch A., Line P., Popovski M., From Testing to
 Codification: Post-tensioned Cross Laminated Timber Rocking Walls, INTER conference, Tacoma WA, 2019.